FROM: Ocean Seismo-Acoustics
ed. T. Akal & J. Berkson
Plenum Press (1986)

GAUSSIAN BEAMS AND 3-D BOTTOM INTERACTING ACOUSTIC SYSTEMS

Homer P. Bucker and Michael B. Porter*

U.S. Naval Ocean Systems Center, Code 541

San Diego, California 92152

ABSTRACT

The analysis of the performance of current array systems requires accurate propagation modeling. In addition, future signal processing algorithms may incorporate a propagation model in order to obtain improved target tracking. The acoustic field received at an array of sensors located on or near the ocean bottom is strongly affected by the local bathymetry and by the physical properties of the ocean subbottom. At very low frequencies, the acoustic field may even be affected by the physical properties of the basement underlying the top sediment layers. This paper describes two techniques based on Gaussian beam tracing for computing the acoustic field in such an environment. The first method employs empirically derived formulas governing the spread of the beams and has the advantage of great simplicity. In the second method the beam curvature and width are obtained formally from an ordinary differential equation along the central ray. This latter method has recently received a lot of attention in the seismological community. Both methods are free of the difficulties at caustics and in shadow zones which afflict standard ray tracing algorithms. Comparisons are presented between the standard ray tracing, simplified beam tracing, formal beam tracing and the exact solution for a difficult negative sound speed gradient problem previously examined by Pedersen and Gordon. Finally, a detection system is proposed that employs Gaussian beam tracing convolved with target tracking.

---

* Now at the Naval Research Laboratory, Washington, D.C. 20375.

INTRODUCTION AND REVIEW

Scientific investigations in bottom interacting acoustic systems dates back to the 1930s. However, a researcher today can begin with the shallow water experiments of Worzel and Ewing [1] and the theoretical analysis of a shallow water sound field in terms of normal modes and a branch line integral by Pekeris [2].

Interest in bottom effects was stimulated in the late 1950s with the introduction of bottom bounce sonar systems. Large experimental programs (Marine Geophysical Survey in U.S. and NAVADO in U.K.) were undertaken to define bottom loss vs. grazing angles at different frequencies and areas of the ocean. Theoretical analysis [3] of the problem showed strong interference effects due to reflections from various sediment layers. Also, it was very difficult to determine bottom losses at low grazing angles because of sound paths that refract back into water because of strong gradients in the sediment. It eventually became clear that it is better to describe bottom interaction by a geoacoustic model that details the true thickness and properties of the sediment and rock layers in the real sea floor. The general subject of geoacoustic modeling (with compilation of many measured values) was recently summarized by Hamilton [4]. Additional measured properties of sea floor sediments are listed in Hamilton and Bachman [5] and Hamilton et al. [6].

In the late 1960s and 1970s, many of the loose ends of range-independent bottom interacting propagation had been cleaned up and range-dependent propagation models had been introduced. Special note might be given to shallow water work of Hastrap [7] and Akal [8] at SACLANTCEN. Also, the work (mostly theoretical) by Vidmar [9-12], and others, at the Applied Research Laboratory, University of Texas, has delineated many effects of bottom interaction associated with shear waves in the sediment layers. Work on range dependent models with bottom interaction is represented by papers by Jensen and Kuperman [13] and McDaniel and Lee [14]. An equivalent bottom algorithm was developed by Bucker [15] so the very fast split-step parabolic equation of Tappert [16] can be used in cases with strong bottom interaction.

Finally, any review should include the proceedings of two workshops on bottom interaction. They are the Physics of Sound in Marine Sediments, ed. by Hampton [17] and Bottom Interacting Ocean Acoustics [18], ed. by Kuperman and Jensen.

SOUND PROPAGATION WITH 3-D BATHYMETRY

There are many ways to calculate the sound field with bottom interaction associated with 3-D bathymetry: coupled normal modes, adiabatic mode theory, 3-D parabolic equation models, finite difference or finite element algorithms, etc. In this section the Gaussian beam method will be presented because it generates accurate solutions using an algorithm of moderate complexity and reasonable computation times.

Beam tracing has recently received a great deal of attention for solving problems in seismic wave propagation. Many articles on beam tracing may be found in the October 1984 issue of the Geophysical Journal of the R. astr. Soc. In beam tracing, the radiated field of a source propagates as a fan of Gaussian beams. These beams move through the medium with the central ray of the beam following ray acoustics.

Each beam will have some influence at any receiver point. However, the influence falls off rapidly as the receiver becomes distant from the central ray of each beam, so only beams that pass "near" the receiver will have a noticeable affect.

Standard ray tracing often gives reasonable results, even at low frequencies, in bottom interaction problems. However, there are certain artifacts such as perfect shadows and caustics. These problems are greatly compounded when reflections from a three-dimensional ocean bottom must be considered.

The recent interest in beam tracing stems from the fact that it requires only slight modifications to standard ray tracing codes and because the field solutions are free of singularities at caustics. The modifications to codes that use dynamic ray tracing are so simple as to suggest a close relationship between ray tracing and beam tracing. In fact Deschamps [19] and Felsen [20] show that in some cases bounded beam equations can be obtained by displacing the rays into complex space and using their projection in real space. In the following sections the Gaussian beam solution for a case of unnaturally strong downward refraction (discussed by Pedersen and Gordon [21]) will be compared to standard ray theory and normal mode solutions.

SIMPLE GAUSSIAN BEAMS

An older semi-empirical method, simple Gaussian beams (SGB), used with the Ray-wave 2-D propagation model [22] will be presented first.

Consider one of a fan of beams radiating from a point source as shown in Fig. 1. The beam is traced from the source at 0 to a point P which is in the vicinity of a receiver at R. The contribution to the intensity at R due to the beam is

$$I = A \exp(-a\theta^2)/s^2, \qquad (1)$$

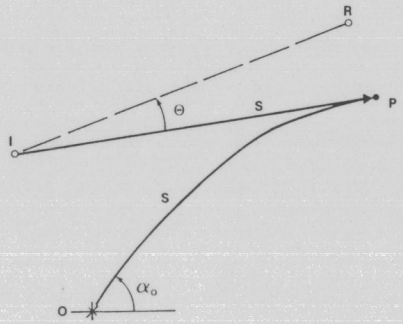

Figure 1. Simple Gaussian Beam.

where A represents the initial strength of the beam, s is the distance along the beam from 0 to P, θ is the angle between $\overline{IP}$ and $\overline{IR}$ (θ is not usually in the plane of the paper in the 3-D case), and "a" determines the fall-off of influence of the beam and is a function of frequency. The phase of the field at R is calculated by extension of the phase of the beam at P assuming a spherical wave front centered at image point I. Point I is located by extending a line, tangent to the beam at P, back a distance s. When the beam interacts with a boundary, there are usual changes to the strength, A, and to the phase.

Because the beam width parameter "a" does not change when the simple beam passes through the refracting ocean or sediments, it is necessary to first group together beam contributions of the same type. Then a complex pressure is calculated for each group and these are added to give the total field. For example, assume that there are contributions from three direct (D) beams with intensity I_1, I_2, I_3 and phase ϕ_1, ϕ_2, ϕ_3 and two surface reflecting (SR) beams (I_4, I_5) with phase ϕ_4, ϕ_5. Note that $\phi_1 \approx \phi_2 \approx \phi_3$ and $\phi_4 \approx \phi_5$. First calculate "complex group intensities"

$$I_D = \sum_{m=1}^{3} I_m \exp(i\phi_m) \text{ and } I_{SR} = \sum_{m=4}^{5} I_m \exp(i\phi_m). \tag{2}$$

Then the total complex pressure is

$$p = |I_D|^{\frac{1}{2}} \exp[i \arg(I_D)] + |I_{SR}|^{\frac{1}{2}} \exp[i \arg(I_{SR})]. \tag{3}$$

To determine the type of a beam, a group identification number (ID) is calculated as the beam propagates. An ID = 0 indicates that the beam has not yet been affected by any of the following: surface reflection, turn-over, turn-under, bottom reflection, touching a caustic. When the beam has a surface reflection, the number 2 is concatenated with the previous ID (a leading 0 can be omitted). A number 4, 6, or 8 is added for a turn-over, turn-under, or bottom reflection. When the central ray touches a caustic, the last number is increased by 1. For example, a ray ID = 294 would indicate that the beam had a surface reflection, a bottom reflection, touched a caustic, and then a turn-over. When beam splitting (e.g., part of a beam may reflect from an interface with part traveling through) occurs, the calculation must be done in several passes with only one type of action (e.g., the reflection) taking place during each pass.

GAUSSIAN BEAM EQUATIONS

A readable development of Gaussian beam (GB) equations is given by Červený et al. [23]. The GB equations are developed relative to a central ray that obeys standard ray equations. Consider first the 2-D Cartesian coordinate system (x, z) and let s represent a distance measured along the central ray.

The GB curvature and beam width are derived from auxilliary variables p(s) and q(s) which are obtained by integrating a pair or ordinary differential equations along the central ray,

$$dq/ds = c(s)p(s), \text{ and } dp/ds = -c_{2N}q(s)/c^2(s). \tag{4}$$

Here c(s) is the sound speed at a point s units along the ray path and c_{2N} is the second derivative of the sound speed normal to the central ray.

In order to solve these equations, the initial conditions p(0) and q(0) must be specified. The final solution depends only on the ratio p(s)/q(s). Therefore, the beam is characterized by a single complex constant $\Gamma = p(0)/q(0)$. This beam constant controls both the initial beam width and curvature and may be chosen in various ways. The optimal procedure for selecting Γ and other parameters of the beam solution (no. of beams, angular spread, etc.) is a matter of current research.

Once p and q are determined, the field due to the beam is given by

$$u(s, \Gamma) = A[(c(s)\, q(0))/(c(0)q(s))]^{\frac{1}{2}}$$

$$\cdot \exp\{i\omega[\tau + p(s)\rho^2/(2q(s))]\}, \tag{8}$$

where A is a source constant to be determined, q(0) and c(0) are values of q and c at the source, ρ is the normal distance from the central ray to the field point, ω is the angular frequency of the source and $\tau(s)$ is the phase delay (travel time) which satisfies the equation

$$d\tau/ds = 1/c(s) \tag{9}$$

EXPANSION OF POINT SOURCE INTO BEAMS

Some sources naturally give rise to Gaussian beams in a particular coordinate system. In other cases the appropriate superposition of beams must be determined. A canonical case for underwater acoustics is a point source in cylindrical coordinates. One approach is to match the high- frequency asymptotic field of the Gaussian beam representation to the exact solution in a homogeneous medium. The Gaussian beam representation is [23]

$$u(x, z) = \int A(\alpha) u_\alpha(s,\rho) d\alpha, \tag{10}$$

where

$$u_\alpha = [q(0)c(s)/(q(s)c(0))]^{\frac{1}{2}}$$

$$\cdot \exp\{i\omega[\tau + p(s)\rho^2/(2q(s))]\}, \tag{11}$$

and α is the grazing angle of the beam at the source.

In the high-frequency limit ($\omega \to \infty$) the method of stationary phase yields the asymptotic representation.

$$u(x, z) \sim A(\alpha_o)[2\pi c(0)/(\omega r)]^{\frac{1}{2}} \exp[i(\omega r/c(0) - \pi/4)] \quad (12)$$

In the above, x is horizontal range, z is depth, and r is the slant distance between the source point and the receiver point. It follows directly that for point-source in two dimensions (line source in 3-D) that

$$A(\alpha_o) = 1/\pi \quad \text{(point source in 2-D)} \quad (13)$$

and that, less formally,

$$A(\alpha_o) = [\omega/(2\pi r c(0))]^{\frac{1}{2}} \exp(i\pi/4) \quad (14)$$

for a point source in 3-D coordinate system with axial symmetry.

REFLECTION AND TRANSMISSION AT INTERFACES

The reflection and transmission of beams at interfaces has been extensively discussed in the literature. Reflection from an elastic medium is complicated and a matter of current research. Cervený and Pšenčík [25] provide complete equations for the case of a first-order curved acoustic interface but their results do not show the expected beam displacement. Felsen [20] discusses this point and suggests that the complex angle of the associated complex ray should be used in the equations. Until this matter is resolved, displacement of the central beam, as discussed by Tindle [26], will probably yield acceptable results.

COMPARISON OF ALGORITHMS

It is reasonably clear that there is a smooth extension of the Gaussian beam algorithms from two to three dimensions. Therefore, a useful check on the algorithms is a two dimensional problem with very strong gradient effects. The profile used has a single negative gradient layer ($c(z)^{-2} = a + bz$) with sound speed equal to 1677.33 yds/sec (1 yd = 0.9144 m) at the surface and equal to 1068.33 yds/sec at a depth of 1000 yds. Obviously, this gradient is much stronger than any that occurs naturally over a water layer with a few meters, or greater, thickness. This profile was studied by Pedersen and Gordon [21] in a comparison of ray and normal mode solutions.

Fig. 2 is a ray plot for a frequency = 2 kHz and a source depth at 66.7 yds. The level will be calculated for a receiver at the same depth and at various ranges. Fig. 3 is a comparison of the ray theory solution and a SGB solution with 0.2° beam spacing and a = 1.E+6, and Fig. 4 is a comparison of the normal mode solution (with 100 modes) and the SGB solution. At ranges less than ~570 yds the mode solution is not correct because of an insufficient number of modes. It is clear that for this extremely difficult test the SGB algorithm is the best of the three methods overall giving essentially exact results from 0 to 760 yds with a reasonable fit to the mode theory beyond 760 yds. Fig. 5 is a plot of the GB algorithm with a 0.225° beam spacing and the normal mode solution.

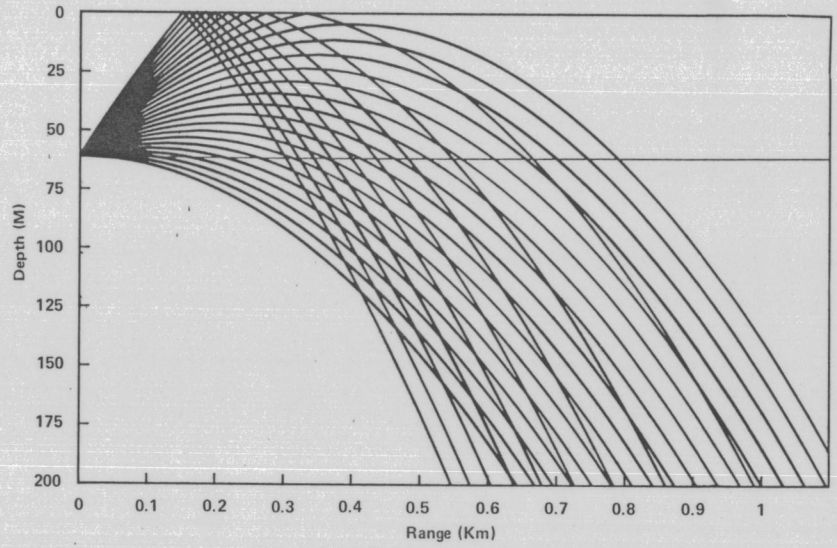

Figure 2. Ray Plot for Shallow Source.

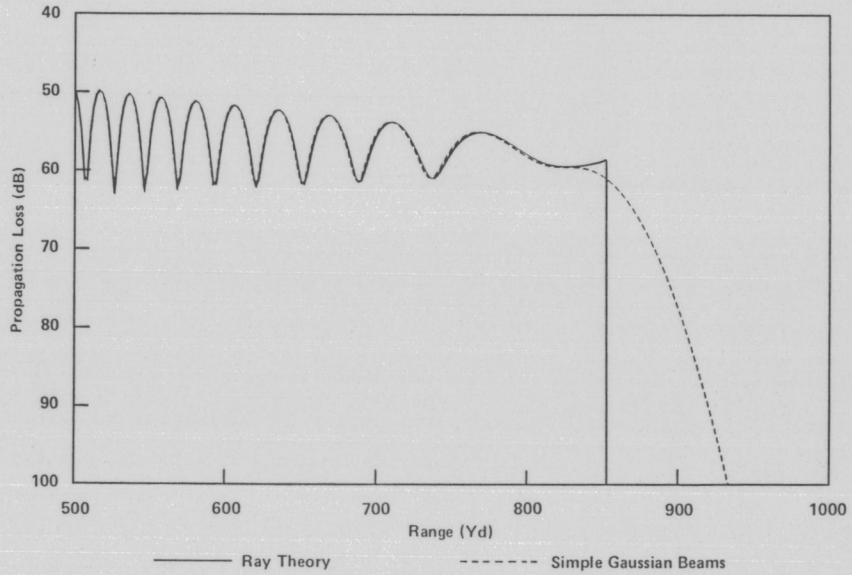

Figure 3. Comparison of Ray Theory and SGB Algorithm.

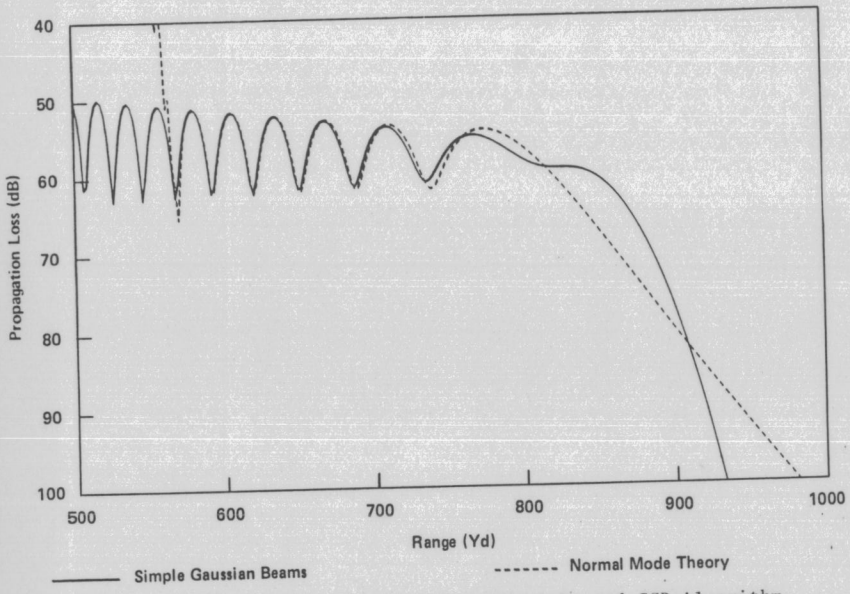

Figure 4. Comparison of Normal Mode Algorithm and SGB Algorithm.

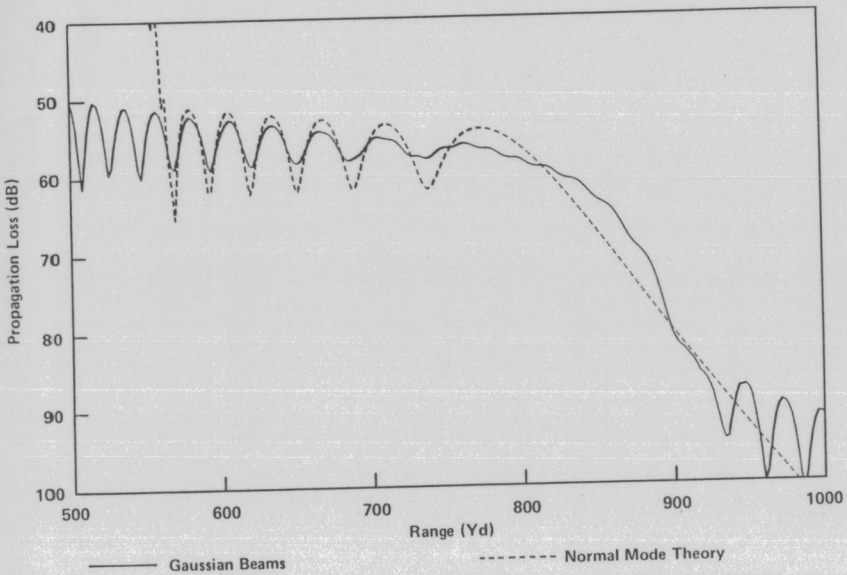

Figure 5. Comparison of Normal Mode Algorithm and GB Algorithm.

A second example is taken from Pedersen and Gordon where the source is at 1000 yds and the receiver at 800 yds. A range interval from 3100 to 3170 yds is examined. Over the interval the situation changes from interference between a downward refracted and a surface reflected ray, to interference between two downward refracting rays (one of which has touched a caustic), to a caustic (at 3158.8 yd), and to the shadow zone beyond the caustic. For this deep source it is not possible to examine the normal mode solution because of numerical problems. Fig. 6 is a comparison of a SGB solution with a 0.15° beam spacing and the ray theory solution. The small beam spacing is a consequence of the extreme gradient. Typically, beam spacings of 1° or so are suitable. Fig. 7 is a comparison of the SGB algorithm and the GB algorithm with a beam spacing of 0.18°.

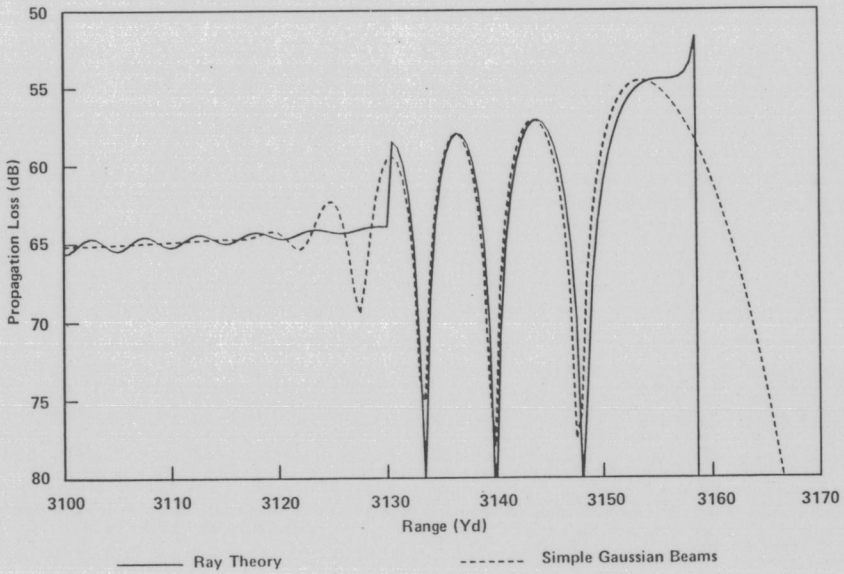

Figure 6. Comparison of Ray Theory and SGB Algorithm for Deep Source.

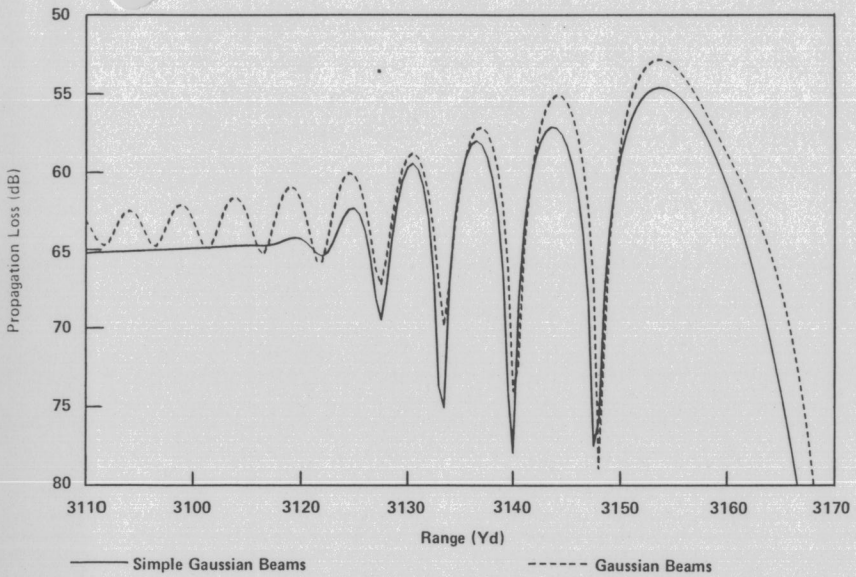

Figure 7. Comparison of SGB Algorithm and GB Algorithm for Deep Source.

GAUSSIAN BEAMS AND ACOUSTIC ARRAYS

To illustrate how bottom interaction affects an acoustic array, the bottom bathymetry shown in Fig. 8 is modeled. Fig. 9 is a blow-up of the bathymetry showing an 8 sensor line array (with 15 m separation) lying on the bottom. The 3-D Gaussian beam algorithm is used to calculate the field near the array and a normal mode (or parabolic equation) algorithm extends the field from the 3-D solution to a distant point.

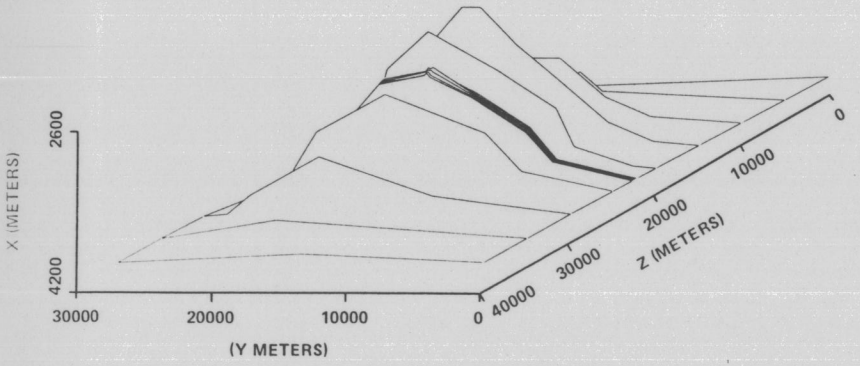

Figure 8. Model of Bottom Topology.

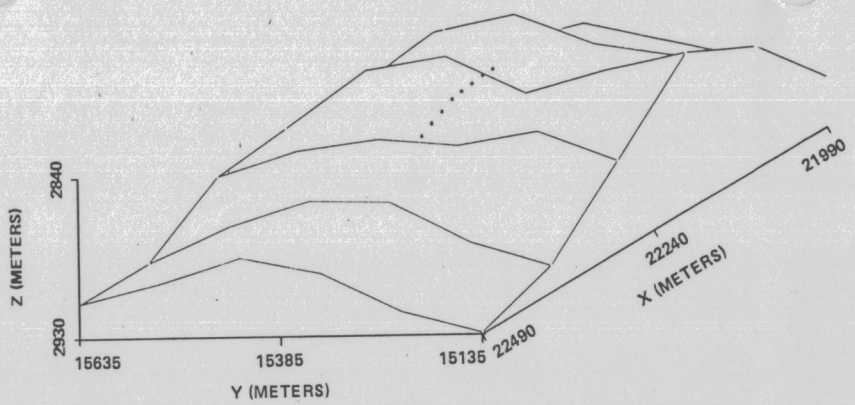

Figure 9. Close-up of Bottom Topology with Line Array.

In standard beam forming, a beam in look direction $\hat{\phi}$ is the dot product of the received signal $\vec{F}(F_1, F_2, \cdots F_N)$ and the expected signal $\vec{f}_{\hat{\phi}}(f_1, f_2, \cdots f_N)$, where $f_j = \exp[i(kx_j \cos\hat{\phi})]$, and x_j = location of the j^{th} sensor in a line array. The beam output is squared and time averaged to stabilize the direction estimate $D_{\hat{\phi}}$. That is,

$$B_{\hat{\phi}} = \Sigma_j \, f_j^* \, F_j \text{ and } D_{\hat{\phi}} = \langle B \, B^* \rangle, \tag{15}$$

where * denotes complex conjugate and $\langle \cdot \rangle$ a time average.

Fig. 10 shows the direction estimate $D_{\hat{\phi}}$ for a signal coming from 90° as a function of the range to the target. The actual range is 94 km and the source frequency is 46 Hz. The array is seen to have good performance, in general.

In matched field processing [27], the reference functions (f_j in Eq. 15) are calculated for an assumed range, bearing, and depth of the target. In this case, D becomes $D_{\hat{\phi},r,z}$ where r and z are the range and depth of the target. Fig. 11 is a plot of D as a function of $\hat{\phi}$ and r with z held fixed at the depth (91 m) of the target. Fig. 11 shows, as one might have deduced from the stable beam patterns of Fig. 10, that the array has very little range resolution. Range resolution can be improved by adding one or more sets of sensors above the set on the bottom. That is, each bottom sensor is replaced by a vertical line of sensors forming a billboard array. Fig. 12 shows the value of $D_{\hat{\phi},r,z}$ as a function of r for $\hat{\phi}$ and z equal to the bearing and depth of the target. The different curves correspond to different numbers of sensors (with 2 wavelength spacing) on the eight vertical lines.

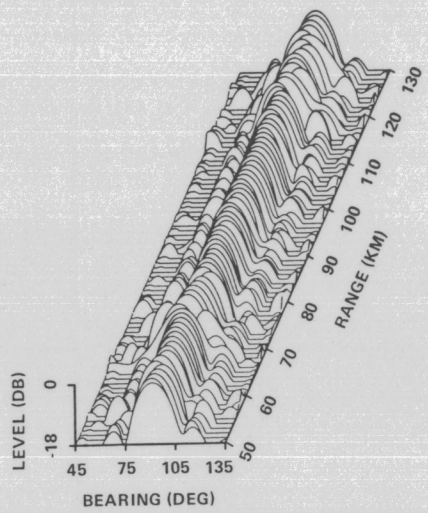

Figure 10. Direction Estimates as a Function of Range.

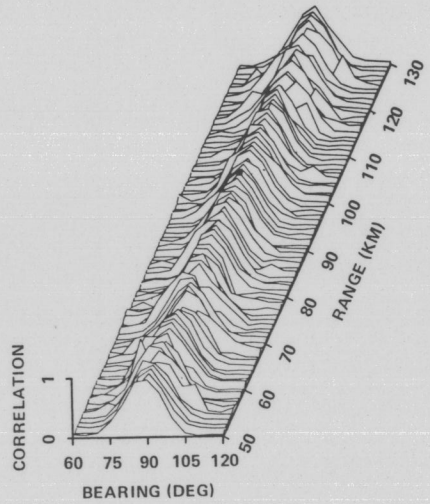

Figure 11. $D\hat{\Phi},r,z$ as a Function of $\hat{\Phi}$ and r,z = const.

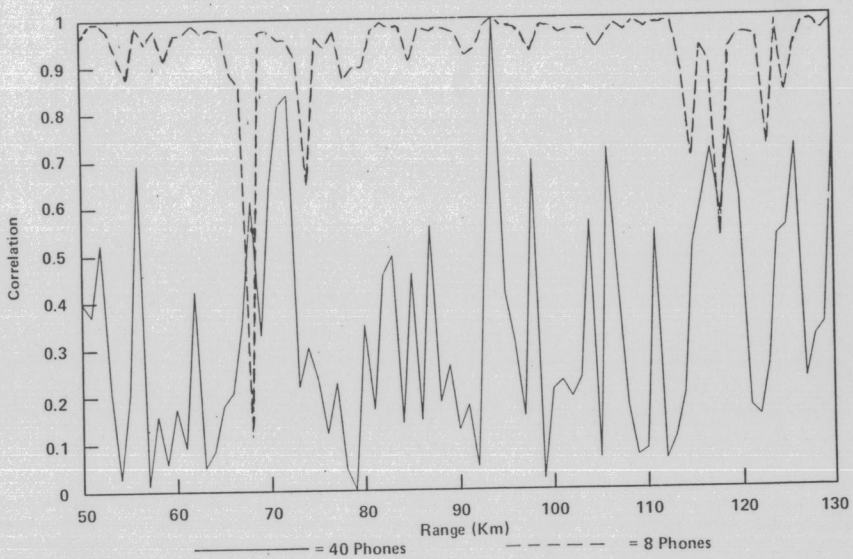

Figure 12. $D\hat{\Phi},r,z$ as a Function of r for Different Number of Sensors on 8 Vertical Lines.

The above procedure applies to a one time look at the signal field. Significant processing gains should result from tracking the peaks of $D_{\hat{\Phi},r,z}$ as a function of time while incorporating known characteristics of possible targets. This is called SMART processing (an acronym for Signals + Model of Acoustic Response + Tracking). There are myriad ways to organize a SMART processor, but the best performance will probably come from extending the time span of the coherent detection function (D) as long as possible.

CONCLUSION

Although the algorithms discussed in this paper are simple, they present a considerable computation burden when complex bathymetry is treated in three-dimensions. Certainly, at some frequencies, depending upon the location, there is too much scattering for the algorithms to work. Also it may not be feasible to gather the relevant environmental data. On the other hand, the ocean bottom is essentially constant, unlike the changing water column. Thus, bottom parameters can be collected over a long period of time and the propagation models can be improved by comparisons with experimental data.

For a long time, acousticians have wanted to incorporate their propagation models into signal processing. With the advent of efficient models and low cost computing machines, this may soon be done.

ACKNOWLEDGEMENTS

Support for this effort was provided by the NAVOCEANSYSCEN Independent Research Program and the Bottom Interaction Program at NORDA. Calculations for the matched field figures were done by Philip Schey, CSC Corp.

REFERENCES

1. J. L. Worzel and M. Ewing, Explosion sounds in shallow water, Section I, pp. 1-53 in Geological Society of America, Memoir 27, (1948).

2. C. L. Pekeris, Theory of propagation of explosive sound in shallow water, Sect. II, pp. 1-117 in Geological Society of America, Memoir 27 (1948).

3. H. P. Bucker, J. A. Whitney, G. S. Yee and R. S. Gardner, "Reflection of low frequency sonar signals from a smooth ocean bottom," J. Acoustic Soc. America, No. 37, pp. 1037-1051 (1965).

4. E. L. Hamilton, "Geoacoustic modeling of the sea floor," J. Acoustic. Soc. Am., No. 68, pp. 1313-1340 (1980).

5. E. L. Hamilton and R. T. Bachman, "Sound velocity and related properties of marine sediments," J. Acoustic. Soc. Am., No. 72, pp. 1891-1904 (1982).

6. E. L. Hamilton, R. T. Bachman, R. T. Berger, W. R. Johnson and L. A. Mayer, "Acoustic and related properties of calcareous deep-sea sediments," J. Sedimentary Petrology, No. 52, pp. 733-753 (1982).

7. O. F. Hastrup, "Some bottom-reflection loss anomalies near grazing and their affect on propagation in shallow water," pp. 135-152 in Ref. 18.

8. T. Akal, "Sea floor affects on shallow-water acoustic propagation," pp. 557-575 in Ref. 18.

9. K. E. Hawker, "The existence of Stoneley waves as a loss mechanism in plane wave reflection problems," J. Acoustic Soc. Am., No. 65, pp. 622-686 (1979).

10. P. J. Vidmar, "Ray path analysis of sediment shear wave affects in bottom reflection loss," J. Acoust. Soc. Am., No. 68, pp. 639-648 (1980).

11. H. Holthusen and P. J. Vidmar, "The affect of near-surface layering on the reflectivity of the ocean bottom," J. Acoust. Soc. Am., No. 72, pp. 226-234 (1982).

12. R. A. Koch, P. J. Vidmar, and J. B. Lindberg, "Normal mode identification for impedence boundary conditions," J. Acoust. Soc. Am., No. 73, pp. 1567-1570 (1983).

13. F. B. Jensen and W. A. Kuperman, "Sound propagation in a wedge shaped ocean with a penetrable bottom," J. Acoust. Soc. Am., No. 67, pp. 1564-1566 (1980).

14. S. T. McDaniel and D. Lee, "A finite-difference treatment of interface conditions for the parabolic equation," J. Acoust. Soc. Am., No. 71, pp. 855-858 (1982).

15. H. P. Bucker, "An equivalent bottom for use with the split-stop algorithm," J. Acoust. Soc. Am., No. 73, pp. 486-491 (1983).

16. F. D. Tappert, "The parabolic equation method," Sect. V in Lecture Notes in Physicis, No. 70, Ed. by J. B. Keller and J. S. Papadakis, Springer Verlag, Berlin, 1977.

17. Physics of Sound in Marine Sediments, ed. by Loyd Hampton, Plenum Press, New York, 1974.

18. Bottom Interacting Acoustics, ed. by W. Kuperman and F. Jensen, Plenum Press, New York, 1980.

19. G. A. Deschamps, "Gaussian beams as a bundle of complex rays," Electronics Letters, No 7, pp. 684-685 (1971).

20. L. B. Felsen, "Geometrical theory of diffraction, evanescent waves, complex rays and Gaussian beams," Geophys. J. R. astr. Soc., No. 79, pp. 77-88 (1984).

21. M. A. Pedersen and D. F. Gordon, "Normal-mode and ray theory applied to underwater acoustic conditions of extreme downward refraction," J. Acoust. Soc. Am., No. 51, pp. 323-368 (1971).

22. H. P. Bucker, "Some comments on ray theory with examples from current NUC ray trace models," pp. 32-36 in SACLANT Conf. Proceed., No. 5, (1971).

23. V. Červený, M. M. Popov, and I. Pšenčík, "Computation of wave fields in inhomogeneous media-Gaussian beam approach," Geophys. J. R. astr. Soc., No. 70, pp. 109-128 (1982).

24. L. Klimes, "Expansion of a high frequency time-harmonic wavefield given on an initial surface into Gaussian beams," Geophys. J. R. astr. Soc., No. 79, pp. 105-118 (1984).

25. V. Červený and I. Pšenčík, "Gaussian beams in elastic 2-D laterally varying structures," Geophys. J. R. astr. Soc., No. 78, pp. 65-91 (1984).

26. C. T. Tindle, "Ray calculations with beam displacements," J. Acoust. Soc. Am., No. 73, pp. 1581-1586 (1983).

27. H. P. Bucker, "Use of calculated fields and matched-field detection to locate sound sources in shallow water," J. Acoust. Soc. Am., No. 59, pp. 368-373 (1976).